Self-Assembly

International Edition: DOI: 10.1002/anie.201500292
German Edition: DOI: 10.1002/ange.201500292

Self-Discriminating Termination of Chiral Supramolecular Polymerization: Tuning the Length of Nanofibers**

Jatish Kumar, Hiroyuki Tsumatori, Junpei Yuasa, Tsuyoshi Kawai, and Takuya Nakashima**

Abstract: *Directing the supramolecular polymerization towards a preferred type of organization is extremely important in the design of functional soft materials. Proposed herein is a simple methodology to tune the length and optical chirality of supramolecular polymers formed from a chiral bichromophoric binaphthalene by the control of enantiomeric excess (ee). The enantiopure compound gave thin fibers longer than a few microns, while the racemic mixture favored the formation of nanoparticles. The thermodynamic study unveils that the heterochiral assembly gets preference over the homochiral assembly. The stronger heterochiral binding over homochiral one terminated the elongation of fibrous assembly, thus leading to a control over the length of fibers in the nonracemic mixtures. The supramolecular polymerization driven by π–π interactions highlights the effect of the geometry of a twisted π-core on this self-sorting assembly.*

The past two decades have witnessed increased attention in the field of the self-assembly of small molecules into complex architectures.[1] This interest in supramolecular polymers formed by noncovalent interactions arises mainly because of a) the desire to mimic life systems so as to understand the process of self-assembly in biological macromolecules[2a] and b) the ability to build nanostructures for practical applications by utilizing a bottom-up approach.[2b–d] The bottom-up approach drives the formation of supramolecular aggregates through a combined effect of different noncovalent intermolecular forces, thus leading to complex superstructures, often possessing a fibrous nature.[3] Molecules possessing chiral centers act as building blocks for the fabrication of helical nanostructures, wherein the supramolecular chirality is determined by the chirality at the molecular level.[4,5] The fascinating structural features of different chiral nanostructures, such as helices, nanotapes, and nanotubes have attracted great interest because of their resemblance to biological structures[6a] and possible applications in chiral sensing and catalysis.[6b–d]

[*] Dr. J. Kumar, Dr. H. Tsumatori, Dr. J. Yuasa, Prof. T. Kawai, Dr. T. Nakashima
Graduate School of Materials Science
Nara Institute of Science and Technology (NAIST)
8916-5 Takayama, Ikoma, Nara 630-0192 (Japan)
E-mail: tkawai@ms.naist.jp
ntaku@ms.naist.jp

[**] We are most grateful to S. Fujita for the cryo-TEM measurements. This work was supported in part by the Grand-in-Aid for Scientific Research (No. 25248019) from JSPS. J.K. also acknowledges JSPS for the post-doctoral fellowship.

Supporting information for this article is available on the WWW under http://dx.doi.org/10.1002/anie.201500292.

The performance of functional organic materials in optoelectronic devices is largely dependent on the organization of molecular components.[6] Hence, directing the self-assembly towards a preferred type of organization is an extremely important step in the design of such materials. Recently, we reported the self-assembly of chiral binaphthalenes, bearing two perylene bis(imide) (PBI) units (**1**; Scheme 1),[7] into dissimilar morphologies depending on the solvent system.[8] They formed helical fibers through π–π stacking interactions in methylcyclohexane (MCH), but formed spherical aggregates in chloroform at high concentration.[8] The fibrous assemblies gave superior chiroptical properties, including circularly polarized luminescence (CPL) relative to the spherical aggregates. In the present work, we introduce a new methodology to control the length of the fibers through the mixing of enantiomers possessing the opposite chirality. In this regard, earlier investigations have demonstrated the morphological changes of fibrous assemblies[9] with supramolecular chirality following the "majority rules" effect,[10] or the chiral self-sorting during self-organization.[11] Although most studies in which the *ee* values were varied, morphological changes of the fibers resulted, to the best of our knowledge, no example of control on the assembly length has been reported without changing morphology. Herein, we utilize enantiomeric mixing for controlling the length as well as the supramolecular chirality of supramolecular polymers.

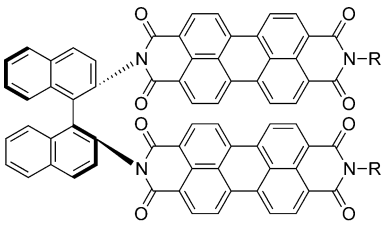

(*S*)-**1**

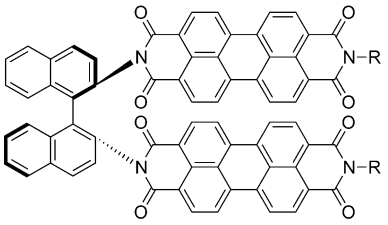

(*R*)-**1**

Scheme 1. Molecular structure of the *S* and *R* isomers of **1** [R = CH-$(C_6H_{13})_2$].

We first examined the racemic coassembly of **1**. Freshly prepared solutions of *S* and *R* isomers in chloroform/MCH (1:49) at a concentration of 1×10^{-5} M, wherein they form extended fibers,[8] were mixed at room temperature. The solution mixture was then annealed above 95 °C with subsequent slow cooling to room temperature at a rate of 1 °C min^{-1}. The TEM image before annealing (Figure 1 A)

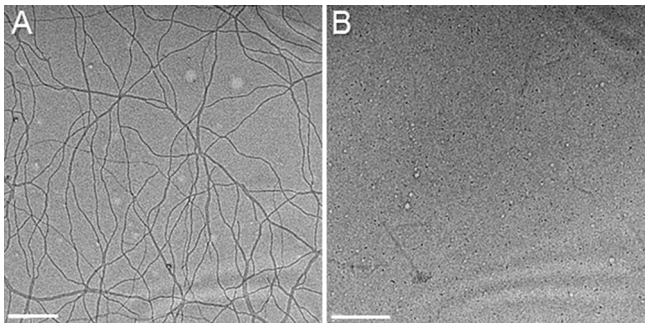

Figure 1. TEM images of racemic coassembly of (*R*)- and (*S*)-**1** before (A) and after (B) annealing at 95 °C. Scale bar = 200 nm.

suggested that the fibers formed from enantiopure isomers remain phase separated. After annealing, the fibrous assemblies completely disappeared and ill-structured nanoparticles with a diameter of 10–20 nm were formed (Figure 1 B). Similar behavior was earlier observed in the self-assemblies driven by π–π stacking interactions of core-twisted π-systems including helicene derivatives[12] and bay-substituted PBIs.[13] The injection of chloroform solutions of **1** into MCH provided similar results without annealing. The solution of the pure enantiomer gave the extended fibers, while nanoparticles were obtained by the injection of a chloroform solution of premixed racemate (see Figure S1 in the Supporting Information). This fact indicated that annealing disassembled the aggregates into their monomeric state, just as if it was dissolved in chloroform, and both the fibrous and particulate aggregates could be assembled from the identical monomeric state.

The mechanistic studies on supramolecular polymerization have been well-documented and are based on the isodesmic and cooperative models.[14] Würthner and co-workers described that the simple assemblies of PBI dyes through π–π interactions, as in our present case, were fitted well by the isodesmic model.[15] In the isodesmic model, each step of the monomer attachment to the chain-end is governed by a single equilibrium constant, K_I. Temperature-dependent absorption studies showed a sigmoidal curve for the fraction of aggregates versus temperature, thus suggesting an isodesmic model in both cases (Figure 2 A). Similar fits were observed in temperature-dependent CD analyses (see Figure S2 in the Supporting Information). A gradual disassembly profile was observed upon addition of chloroform to the aggregates, thus confirming the isodesmic mechanism (see Figure S3 in the Supporting Information).[16] These studies also suggested that the racemic aggregates were more stable than the enantiopure fibers. Nonlinear least-square regression analysis of the concentration-dependent absorption spectra[15b] showed that

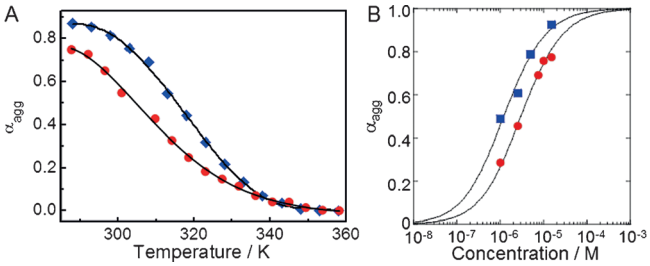

Figure 2. Fraction of aggregated molecules (α_{agg}) as a function of temperature (A) and total concentration of **1** (B), in a mixture of chloroform/MCH (1:49), as obtained by fitting the apparent absorption coefficients at $\lambda = 522$ nm to the isodesmic model for enantiopure (red circles) and racemic solution (blue squares). Also see Figure S4 and the footnotes.

the assembly behavior can be described well by the isodesmic model (Figure 2 B) for the homochiral supramolecular polymers. The association constant at room temperature was determined to be $K_{homo} = (2.0\pm0.1\times10^5)\,M^{-1}$. The apparent association constant for the racemic aggregates was also roughly determined by this model to be $K_{rac} = (4.9\pm0.5\times10^5)\,M^{-1}$. Since the homochiral interaction is also possible, even if it is not very likely, in the solution of the racemates, the practical heterochiral association constant (K_{hetero}) could be larger than the K_{rac} value, which apparently leads to the larger K_{hetero} versus K_{homo} value. In addition to the result in Figure 1, the mechanistic study indicated two important characteristics of the assemblies: a) The enantiopure compound forms fibrous assemblies, while the racemic mixture favors the nonfibrous nanoparticles (Scheme 2), and b) the formation of racemic nanoparticles is thermodynamically favored over the homochiral fibers, thus demonstrating that self-discrimination prevails over self-recognition.

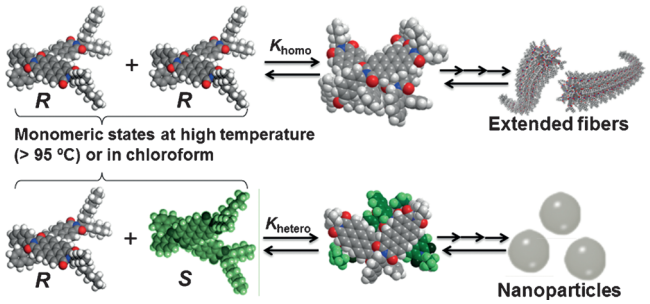

Scheme 2. Schematic illustration of the assembly of **1** in homochiral and racemic systems together with dimeric models calculated by MMFFs94.

The absorption spectrum of an MCH solution of the pure enatiomer gave a profile typical of assemblies with helically arranged PBI dyes (see Figure S5 in the Supporting Information).[17] The intense band at $\lambda = 550$ nm in the enantiopure solution shifted to $\lambda = 545$ nm with emergence of a shoulder at $\lambda = 565$ nm for the racemic solution, thus indicating a change in packing arrangement. The rough conformational searches of dimeric models with the MMFF94 s force field using the CONFLEX program[18] gave dissimilar structures (see Fig-

ure S6 in the Supporting Information). The heterochiral dimer showed a complementary stack, while the optimized homochiral dimer had rotationally displaced PBI units (Scheme 2). The heterodimer gave a smaller steric energy than that of the homodimer.

The stronger heterochiral interaction over homochiral one inspired us to control the length of fibers by varying the *ee* value through the self-sorting property in the supramolecular polymerization. The fibrous growth by self-recognition with K_{homo} could be deactivated by the heterochiral interactions which prefer nonfibrous growth. The elongation and deactivation of fibrous growth at the ends are thermodynamically controlled with K_{homo} and K_{hetero}, respectively. Meanwhile, the probabilities of homochiral and heterochiral interactions should be stochastically controlled by *ee* values, and would lead to the controlled persistent homochiral growth of fibers. The length of supramolecular polymers is usually controlled by varying temperature, concentration, and solvent composition.[14a] In this context, recently Takeuchi, Sugiyasu, and co-workers succeeded in controlling the length of supramolecular polymers based on porphyrin assemblies with a narrow polydispersity.[19] They employed an interplay of isodesmic and cooperative aggregation pathways to achieve living supramolecular polymerization. The present study is the first attempt to control the length of supramolecular fibers in terms of the *ee* value, or through an interplay of chiral self-recognition and self-discrimination behaviors.

The coassemblies of (*S*)- and (*R*)-**1** with different *ee* values were characterized by SEM [Figure 3 and Figures S7, S8 (TEM), S9 (AFM), and S10 (cryo-TEM) in the Supporting Information]. Very interestingly, the self-assembly at different *ee* values resulted in fibrous structures with varying lengths, and without a change in the morphology and the width of fibers. The enantiopure assembly resulted in extended fibers, which were longer than a few microns with a width of (9 ± 3) nm, after accounting for the AFM tip-broadening factor. The line profile analysis of topographic image obtained by AFM estimated the height of fibers to be about (4 ± 0.5) nm, which almost correspond to a unimolecular length. The length of the fibers decreased with decreasing *ee* value, thus leading to the formation of particles possessing an average diameter of 10–20 nm for the racemic mixture. At the higher *ee* values of 0.8 and 0.9, the nanostructures are composed of longer fibers along with shorter fibers. For *ee* values between 0.8 and 0.2, only shorter fibers could be observed, the lengths of which were sharply dependent on the *ee* value. A histogram of the length distribution of the fibrous structures obtained by measuring 50 fibers shows a clear increase in the length of fibers with increasing *ee* values (Figure 3G). An average length of about (125 ± 20), (275 ± 35), and (490 ± 50) nm was observed for fibers with *ee* values of 0.2, 0.4, and 0.6, respectively (Figures 3B,C,D). A plot of the size of the nanofibers versus the *ee* value gives a parabolic curve, thus suggesting precise control over the length by varying the *ee* values (Figure 3H). It should be noted that the cryo-TEM images directly demonstrated that the length of fibrous assemblies was indeed controlled in the solution state.

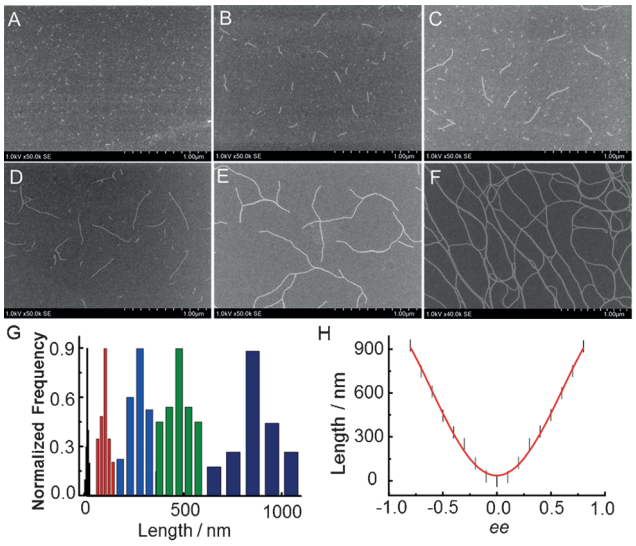

Figure 3. SEM images of coassembly of (*R*)- and (*S*)-**1** at *ee* values of 0.0 (A), 0.2 (B), 0.4 (C), 0.6 (D), 0.8 (E), and 1.0 (F). G) Histogram of the length distribution of nanofibers obtained by measuring 50 fibers for *ee* values of 0.0 (black), 0.2 (red), 0.4 (blue), 0.6 (green) and 0.8 (navy blue). H) A plot of average length of nanofibers versus the *ee* value.

Meanwhile, the nanoparticles coexisted for the samples with *ee* values below 0.6. One may wonder if the racemic portion provided nanoparticles, whereas the remaining enantiopure component self-assembled into short fibers. However, under this assumption, the length of the fiber should depend on the concentration of enantiopure molecules. In contrast, the extended fibers were formed regardless of the concentration (see Figures S11 and S12 in the Supporting Information), thus clearly disproving this assumption. It also appears that a single heterochiral binding does not always terminate the fibrous growth completely. That is, for example, even the mixture of $ee = 0.9$, in which no particles coexisted in the SEM image, contains 5% of the minor enantiomer, wherein the average number of the enantiomer in an uninterrupted homochiral sequence could be only 10.5 under random copolymerization conditions.[20] This number seems small considering the length of the fibers observed. The relatively small difference between the K_{homo} and K_{hetero} values with a similar order of magnitude may tolerate the incorporation of the opposite enantiomer in the fibers. Taking the above discussion into account, there are three possibilities for the minor enantiomer in nonracemic mixtures: to form racemic particles ($ee < 0.6$), be incorporated into the fibers with a nonpreferred screw sense at the cost of mismatch penalty,[21] and terminate the fibrous growth at the ends. Therefore, a certain number of successive heterochial interactions at the growing end may be necessary to terminate the supramolecular polymerization.

We then investigated the change of optical chirality with varying *ee* values. In the absorption spectra, a gradual hypsochromic shift in peak positions, accompanying a slight hypochromic effect, was observed with a decrease in *ee* value (see Figure S5). This result also rules out the possibility of the phase separation between racemic particles and enantiopure fibers for the samples with *ee* values of less than 0.6, but suggests a change in the molecular packing. The self-assembly

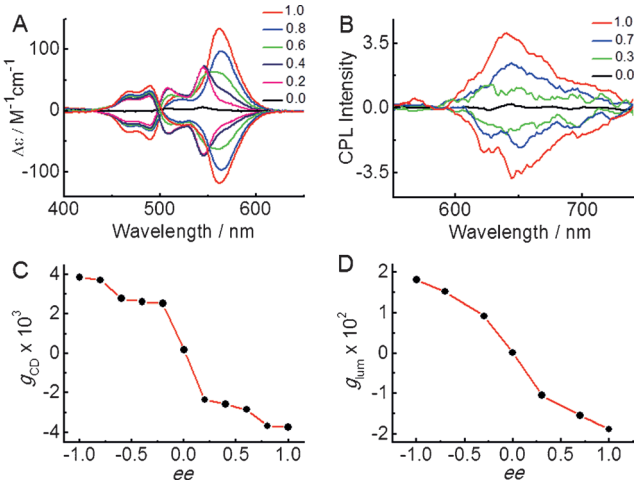

Figure 4. A) CD and B) CPL spectra of the coassembly of (*R*)- and (*S*)-**1** at varying *ee* values. C) Plot of maximum g_{CD} versus *ee* value. D) The g_{lum} value at $\lambda = 640$ nm plotted against the *ee* value.

of the pure components resulted in mirror-image CD profiles with the negative and positive first Cotton effects for the *R* and *S* isomers, respectively, which originate from the supramolecular excitonic interactions in chiral assemblies (Figure 4A).[8] Interestingly, with a decrease in enantiomeric ratio a gradual decrease in the CD intensity of the peak at $\lambda =$ 564 nm was observed with the formation of a new band at $\lambda =$ 546 nm. The CD intensity of this new band for an *ee* value of 0.4 was larger than that for an *ee* value of 0.6, thus indicating a substantial shift in components and molecular ordering responsible for the supramolecular exciton coupling in the self-assemblies. The aforementioned erratic incorporation of the opposite enantiomers in the fibers with a nonpreferred screw sense could lead to a change in the chiral packing mode and the consequent supramolecular chirality. The distinctive chiral bichromophoric geometry in a monomeric component could disrupt the helical arrangement of PBIs when incorporated into a fiber with a nonpreferred screw sense. This effect could cause the more complex CD response with a peak shift relative to other monochromophoric systems complying with the majority-rules effect.[14a,21] The maximum value of the dissymmetry factor (g_{CD}) $\Delta\varepsilon/\varepsilon$ plotted against the *ee* value deviates from linearity, thus suggesting that a certain amount of majority-rules effect was displayed (Figure 4C). For the samples without annealing, a linear fit for the g_{CD} versus *ee* value plot were observed, and is indicative of the fact that the long fibers formed from *S* and *R* isomers remain phase separated before annealing (see Figure S13 in the Supporting Information). That is, the CD intensity at each *ee* value is expressed as the sum of opposite contributions of chiral fibers composed of pure enantiomers.

A gradual quenching in the fluorescence peak at $\lambda =$ 630 nm, thus corresponding to emission from assemblies, was observed with decreasing *ee* values (see Figure S5). The fluorescence quantum yield decreased from a value of 0.45 for an *ee* value of 1.0 to 0.24 for an *ee* value of 0.0 (see Table S1 in the Supporting Information), and a plot of quantum yield against *ee* value showed a sigmoidal fit similar to the CD result (see Figure S14 in the Supporting Information). The molecular ordering for the efficient energy migration is most likely to be disturbed by the heterochiral interactions in the assemblies.[13,22] The CPL spectra exhibited peaks at the corresponding fluorescence wavelengths, the intensity of which decreased with decreasing *ee* values (Figure 4B). The helical fibers of pure components exhibited relatively high CPL activity with a g_{lum} value of 0.02.[8] The sum of cooperative excitonic couplings between the individual components resulted in a remarkably high value of fluorescence dissymmetry for the aggregated structures.[8,22] Similar to the results obtained in the CD profile, a plot of g_{lum} against *ee* exhibited a sigmoidal relationship (Figure 4D). This plot demonstrates a new methodology for the design of self-assembled nanosystems with desired luminescence dissymmetry.

We thus could demonstrate that the length of the fibrous structures, as well as their supramolecular chirality, were sharply dependent on the *ee* value. Successful control could be attributed to the molecular design of **1**, which favors the isodesmic supramolecualr polymerization controlled simply by K_{homo} and K_{hetero} based on the π–π stacking of the twisted cores. The geometry, or the direction of twisting of the core dictated by the axial chirality of binaphthalene unit, therefore, is critical for the growth of assembly through the stacking of cores, and leads to the effective chiral self-sorting.[13] The similar effect of the geometries of twisted π cores was demonstrated by the self-sorting behavior in the dimerization of bay-substituted PBIs,[23] whereas the bichromophoric system is expected to highlight this effect in the present system. The additional introduction of a hydrogen-bonding interactions, which are substantially stronger than π–π interactions, may increase the introduction of the other enantiomers, which can often results in the morphological change of aggregated structures as exemplified in many cases.[9,12]

In conclusion, we have demonstrated the control of the length of supramolecular polymers as well as chiroptical properties of a bichromophoric binaphthalene derivative by varying the *ee* value. The key features of the present system for successfully controlling the length of the supramolecular polymers include the following points: a) The homochiral binding favors the fibrous growth whereas the heterochiral association leads to the nonfibrous assembly, and both events take place under isodesmic conditions, which are simply controlled by K_{homo} and K_{hetero}, respectively; b) The binding constant for the nonfibrous assembly should be larger than that for the fibrous assembly; c) The absence of the hydrogen-bonding interaction emphasizes the effects of the geometry of the twisting bichromophoric π-core in self-assembling processes, thus leading to an efficient self-sorting behavior. The homochiral assembly by self-recognition enabled the fibrous growth, which was efficiently terminated by the heterochiral bindings through the self-discrimination. Although the polydispersity cannot be controlled well through the isodesmic system,[24] these findings still add a new guiding principle for the control of supramolecular polymerization.[14a]

Keywords: chirality · luminescence · polarized spectroscopy · self-assembly · supramolecular chemistry

How to cite: *Angew. Chem. Int. Ed.* **2015**, *54*, 5943–5947
Angew. Chem. **2015**, *127*, 6041–6045

[1] a) S. J. Rowan, S. J. Cantrill, G. R. L. Cousins, J. K. M. Sanders, J. F. Stoddart, *Angew. Chem. Int. Ed.* **2002**, *41*, 898–952; *Angew. Chem.* **2002**, *114*, 938–993; b) M. Figueira-Duarte, K. Müllen, *Chem. Rev.* **2011**, *111*, 7260–7314; c) S. S. Babu, V. K. Praveen, A. Ajayaghosh, *Chem. Rev.* **2014**, *114*, 1973–2129.

[2] a) D. A. Uhlenheuer, K. Petkau, L. Brunsveld, *Chem. Soc. Rev.* **2010**, *39*, 2817–2826; b) S. S. Babu, S. Prasanthkumar, A. Ajayaghosh, *Angew. Chem. Int. Ed.* **2012**, *51*, 1766–1776; *Angew. Chem.* **2012**, *124*, 1800–1810; c) F. Würthner, K. Meerholz, *Chem. Eur. J.* **2010**, *16*, 9366–9373; d) M. R. Wasielewski, *Acc. Chem. Res.* **2009**, *42*, 1910–1921.

[3] R. S. Johnson, T. Yamazaki, A. Kovalenko, H. Fenniri, *J. Am. Chem. Soc.* **2007**, *129*, 5735–5743.

[4] a) M. B. Avinash, T. Govindaraju, *Adv. Mater.* **2012**, *24*, 3905–3922; b) K. Sugiyasu, N. Fujita, S. Shinkai, *Angew. Chem. Int. Ed.* **2004**, *43*, 1229–1233; *Angew. Chem.* **2004**, *116*, 1249–1253; c) L. Zhang, L. Qin, X. Wang, H. Cao, M. Liu, *Adv. Mater.* **2014**, *26*, 6959–6964; d) Y. Yang, Y. Zhang, Z. Wei, *Adv. Mater.* **2013**, *25*, 6039–6049.

[5] a) S. Yagai, S. Mahesh, Y. Kikkawa, K. Unoike, T. Karatsu, A. Kitamura, A. Ajayaghosh, *Angew. Chem. Int. Ed.* **2008**, *47*, 4691–4694; *Angew. Chem.* **2008**, *120*, 4769–4772; b) J. Kumar, T. Nakashima, T. Kawai, *Langmuir* **2014**, *30*, 6030–6037.

[6] a) C. F. Lopez, S. O. Nielsen, P. B. Moore, M. L. Klein, *Proc. Natl. Acad. Sci. USA* **2004**, *101*, 4431–4434; b) J. Hu, W. Kuang, K. Deng, W. Zou, Y. Huang, Z. Wei, C. F. J. Faul, *Adv. Funct. Mater.* **2012**, *22*, 4149–4158; c) H. Peng, L. Ding, T. Liu, X. Chen, L. Li, S. Yin, Y. Fang, *Chem. Asian J.* **2012**, *7*, 1576–1582; d) N. Mizoshita, T. Tani, S. Inagaki, *Adv. Mater.* **2012**, *24*, 3350–3355.

[7] a) H. Langhals, A. Hofer, S. Bernhard, J. S. Siegel, P. Mayer, *J. Org. Chem.* **2011**, *76*, 990–992; b) H. Langhals, *Helv. Chim. Acta* **2005**, *88*, 1309–1343; c) T. Kawai, K. Kawamura, H. Tsumatori, M. Ishikawa, M. Naito, M. Fujiki, T. Nakashima, *ChemPhysChem* **2007**, *8*, 1465–1468; d) H. Tsumatori, T. Nakashima, T. Kawai, *Org. Lett.* **2010**, *12*, 2362–2365.

[8] J. Kumar, T. Nakashima, H. Tsumatori, T. Kawai, *J. Phys. Chem. Lett.* **2014**, *5*, 316–325.

[9] a) R. Oda, I. Huc, M. Schmutz, S. J. Candau, F. C. MacKintosh, *Nature* **1999**, *399*, 566–569; b) D. Berthier, T. Buffeteau, J.-M. Leger, R. Oda, I. Huc, *J. Am. Chem. Soc.* **2002**, *124*, 13486–13494; c) X. Zhu, Y. Li, P. Duan, M. Liu, *Chem. Eur. J.* **2010**, *16*, 8034–8040; d) H. Cao, X. Zhu, M. Liu, *Angew. Chem. Int. Ed.* **2013**, *52*, 4122–4126; *Angew. Chem.* **2013**, *125*, 4216–4220.

[10] a) W. Jin, T. Fukushima, M. Niki, A. Kosaka, N. Ishii, T. Aida, *Proc. Natl. Acad. Sci. USA* **2005**, *102*, 10801–10806; b) A. Lohr, F. Würthner, *Angew. Chem. Int. Ed.* **2008**, *47*, 1232–1236; *Angew. Chem.* **2008**, *120*, 1252–1256; c) M. M. J. Smulders, I. A. W. Filot, J. M. A. Leenders, P. van der Schoot, A. R. A. Palmans, A. P. H. J. Schenning, E. W. Meijer, *J. Am. Chem. Soc.* **2010**, *132*, 611–619; d) M. M. J. Smulders, P. J. M. Stals, T. Mes, T. F. E. Paffen, A. P. H. J. Schenning, A. R. A. Palmans, E. W. Meijer, *J. Am. Chem. Soc.* **2010**, *132*, 620–626.

[11] a) K. Sato, Y. Itoh, T. Aida, *Chem. Sci.* **2014**, *5*, 136–140; b) C. Roche, H. J. Sun, M. E. Prendergast, P. Leowanawat, B. E. Partridge, P. A. Heiney, F. Araoka, R. Graf, H. W. Spiess, X. Zeng, G. Ungar, V. Percec, *J. Am. Chem. Soc.* **2014**, *136*, 7169–7185.

[12] T. Kaseyama, S. Furumi, X. Zhang, K. Tanaka, M. Takeuchi, *Angew. Chem. Int. Ed.* **2011**, *50*, 3684–3687; *Angew. Chem.* **2011**, *123*, 3768–3771.

[13] Z. Xie, V. Stepanenko, K. Radacki, F. Würthner, *Chem. Eur. J.* **2012**, *18*, 7060–7070.

[14] a) T. F. A. De Greef, M. M. J. Smulders, M. Wolffs, A. P. H. J. Schenning, R. P. Sijbesma, E. W. Meijer, *Chem. Rev.* **2009**, *109*, 5687–5754; b) C. Kulkarni, S. Balasubramanian, S. J. George, *ChemPhysChem* **2013**, *14*, 661–673.

[15] a) Z. Chen, V. Stepanenko, V. Dehm, P. Prins, L. D. A. Siebbeles, J. Seibt, P. Marquetand, V. Engel, F. Würthner, *Chem. Eur. J.* **2007**, *13*, 436–449; b) T. E. Kaiser, V. Stepanenko, F. Würthner, *J. Am. Chem. Soc.* **2009**, *131*, 6719–6732.

[16] P. A. Korevaar, C. Schaefer, T. F. A. D. Greef, E. W. Meijer, *J. Am. Chem. Soc.* **2012**, *134*, 13482–13491.

[17] J. M. Lim, P. Kim, M. C. Yoon, J. Sung, V. Dehm, Z. J. Chen, F. Würthner, D. Kim, *Chem. Sci.* **2013**, *4*, 388–397.

[18] H. Goto, E. Osawa, *J. Am. Chem. Soc.* **1989**, *111*, 8950–8951.

[19] a) S. Ogi, K. Sugiyasu, S. Manna, S. Samitsu, M. Takeuchi, *Nat. Chem.* **2014**, *6*, 188–195; b) S. Ogi, T. Fukui, M. L. Jue, M. Takeuchi, K. Sugiyasu, *Angew. Chem. Int. Ed.* **2014**, *53*, 14363–14367; *Angew. Chem.* **2014**, *126*, 14591–14595.

[20] H. J. Harwood, *Angew. Chem. Int. Ed. Engl.* **1965**, *4*, 394–401; *Angew. Chem.* **1965**, *77*, 405–413.

[21] a) J. van Gestel, A. R. Palmans, B. Titulaer, J. A. Vekemans, E. W. Meijer, *J. Am. Chem. Soc.* **2005**, *127*, 5490–5494; b) H. M. ten Eikelder, A. J. Markvoort, T. F. de Greef, P. A. Hilbers, *J. Phys. Chem. B* **2012**, *116*, 5291–5301.

[22] J. Kumar, T. Nakashima, H. Tsumatori, M. Mori, M. Naito, T. Kawai, *Chem. Eur. J.* **2013**, *19*, 14090–14097.

[23] M. M. Safont-Sempere, P. Osswald, M. Stolte, M. Grune, M. Renz, M. Kaupp, K. Radacki, H. Braunschweig, F. Würthner, *J. Am. Chem. Soc.* **2011**, *133*, 9580–9591.

[24] S. A. Schmid, R. Abbel, A. P. Schenning, E. W. Meijer, R. P. Sijbesma, L. M. Herz, *J. Am. Chem. Soc.* **2009**, *131*, 17696–17704.

Received: January 13, 2015
Revised: February 18, 2015
Published online: March 20, 2015

